Large Deflection Analysis of Elastic-Plastic Shells of Revolution

PEDRO V. MARCAL*
Brown University, Providence, R. I.

A finite element method is developed for the large deflection elastic-plastic analysis of axisymmetric shells of revolution. Results were obtained for a torisphere under internal pressure and also for centrally loaded spheres. These results were in reasonable agreement with experiment. A study was made of the effect of elastic-plastic behavior on the buckling of spheres with axisymmetric imperfections subjected to external pressure. It was found that plastic yielding played a significant role in reducing the buckling pressure of these shells. The influence of plastic yielding increased with increase of the thickness to radius ratio.

Introduction

PRESSURE vessels are often subjected to external loads or vacuum loading. An important factor in the design of the main shell structures in such cases is its ability to withstand the external loads without failure due to buckling. These shells are basically axisymmetric in shape and loading and can be analyzed by axisymmetric shell theory.

Large displacement, elastic behavior of the symmetrically loaded shells of revolution, hereafter referred to as shells, is well understood. Computer programs exist for the axisymmetric large displacement and instability of shells.[1-4] Some of these programs even allow for buckling in the asymmetric mode.

Recent experimental[5] and theoretical[1,2] work has shown the importance of axisymmetric imperfections in the buckling of shells subjected to external pressure. Small deviations from the specified geometry can reduce the buckling load by factors greater than two. These investigations have suggested that in the lower ranges of the radius to thickness parameter λ, some yielding occurs in the shell. The use of shells in this region will increase with the operating depth of the submersibles. It is therefore important that the large displacement and instability of shells with plastic yielding be understood. Much less is known about the buckling of elastic-plastic shells. Bijlaard,[6] using a deformation theory of plasticity, found the buckling loads for initially perfect spheres. This was modified heuristically by Krenzke and Kiernan[5] to give better agreement with experiment. To the writer's knowledge, only the buckling of cylinders[7,8] has been considered with an incremental theory of plasticity. Here, the analysis depends on neglect of elastic displacements and the assumption that the shell is only allowed to yield completely through the thickness.

Marcal and his colleagues,[9-12] in a series of papers, have developed a theory for the small displacement behavior of elastic-plastic shells. The differential equations governing the behavior of the shells were solved by a numerical step-by-step integration. The work was aimed at the limited life design of pressure vessels and expansion joints.[13] In general, good correlation was found between theory and experiment. Khojasteh-Bakt[14] has used the finite element method for the elastic-plastic analysis of shells. Reference 14 also investigated the use of different coordinate systems and assumed displacement functions for the shell element. It was found that the curved shell element with a rectilinear coordinate system produced the best results.

Preliminary attempts to use the step-by-step integration method of Ref. 10 met with difficulties in the application of the boundary conditions. The shells of interest were too "long" in the nonlinear region for a numerical integration without segmenting in the manner of Kalnins.[15] At that time, the writer was also developing large displacement finite element methods.[16] It seemed that the most convenient method for the writer to implement a theory was by means of the finite element method. It was therefore decided to adopt a finite element method using the curved shell element with rectilinear coordinates of Khojasteh-Bakht[14] as the starting point. The work then consisted in applying the large deformation theory outlined in general in Ref. 16 to the particular case of a shell of revolution.

The problem may now be stated as follows: 1) to develop a theory for the elastic-plastic large displacement analysis of axisymmetric shells of revolution and implement this in a finite element computer program, 2) to make some comparisons between theory and experiment, and 3) to study the effect of yielding on the behavior of shells with particular reference to spheres with axisymmetric imperfections.

Theoretical Considerations

In this section, we shall first establish the linear incremental stress-strain relation for an elastic-plastic material. Finite element theory for large displacement shell analysis is then developed using these linear relations.

The material behavior is governed by the incremental theory of plasticity and the von Mises yield criterion. It is assumed to work-harden according to an isotropic strain hardening criterion.

Earlier work resorted to the inversion of a matrix because of the need to avoid division by zero in the case of an elastic-perfectly plastic material.[10] However, recent formulations[17,18] have circumvented this and allow the linear incremental relations to be obtained in closed form for all cases of elastic-plastic behavior.

We shall adopt matrix notation for the following formulation of the stress-strain relations. The plastic increment of strain $\{de_p\}$ is given by the normal flow rule of plasticity,

$$\{de_p\} = d\bar{e}_p\{\partial\bar{\sigma}/\partial\sigma\} \tag{1}$$

where $d\bar{e}_p$ is the equivalent plastic strain, $\bar{\sigma}$ is the equivalent yield stress, $\{\sigma\}$ is the stress vector, and the prefix d is used to denote an increment.

The von Mises yield criterion is now written in incremental form

$$[\partial\bar{\sigma}/\partial\sigma]\{d\sigma\} = d\bar{\sigma} = H'd\bar{e}_p \tag{2}$$

Received July 7, 1969; revision received November 26, 1969. The writer is grateful to the Naval Ship Research and Development Center for supporting the research. He is indebted to R. Jones, M. Krenzke, and D. Pincus of that laboratory for many useful discussions. Computing support was provided by the National Science Foundation, Grant GP-4825, in the early stages of the project.

* Associate Professor, Division of Engineering. Member AIAA.

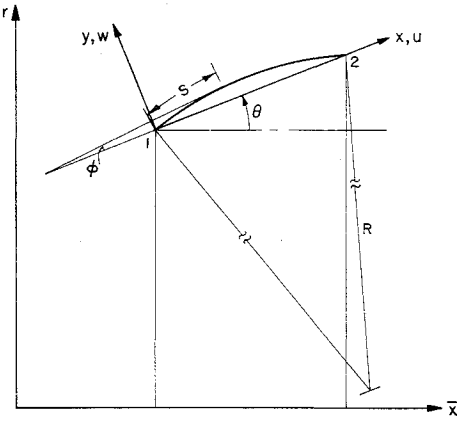

Fig. 1 Axisymmetric shell element.

where H' is the slope of the equivalent stress equivalent strain curve and $\lfloor\ \rfloor$ is used to denote a row vector. Because the elastic components of strains are the only strains that can be associated with changes in stresses, the increment of stress is related to the increment of strain by

$$\{d\sigma\} = [S]\{de_e\} = [S](\{de\} - \{de_p\}) \tag{3}$$

where $[S]$ is the elastic strain to stress transformation matrix, $\{de\}$ is the total increment of strain, and the subscript e is used to denote the elastic component of strain.

By multiplying Eq. (3) by $[\partial\bar{\sigma}/\partial\sigma]$ and using Eqs. (1) and (2), we obtain an expression for the equivalent plastic strain increment $d\bar{e}_p$

$$d\bar{e}_p = \lfloor\partial\bar{\sigma}/\partial\sigma\rfloor[S]\{de\}/(H' + \lfloor\partial\bar{\sigma}/\partial\sigma\rfloor[S]\{\partial\bar{\sigma}/\partial\sigma\}) \tag{4}$$

Substituting for the equivalent plastic strain in Eq. (3) and rearranging, we obtain the required linear incremental stress-strain relation

$$\{d\sigma\} = \left([S] - \frac{[S]\{\partial\bar{\sigma}/\partial\sigma\}\lfloor\partial\bar{\sigma}/\partial\bar{\sigma}\rfloor[S]}{H' + \lfloor\partial\bar{\sigma}/\partial\sigma\rfloor[S]\{\partial\bar{\sigma}/\partial\sigma\}}\right)\{de\} \tag{5}$$

The term† in the bracket of Eq. (5) may be interpreted as the required correction to the elastic stress-strain relation which keeps the stress increment on the expanding yield surface (or tangential to the yield surface in the case of an elastic-perfectly plastic material). An examination of the numerator of the second term in the bracket shows that the term is symmetric. This linear relation is, of course, the same relation as that found previously in the earlier works (Refs. 10, 19, and 20).

Implementation of the Incremental Stress-Strain Relations

In order to reduce the number of load increments required in a solution, we make use of the idea of a transition region[12] where the elastic and elastic-plastic stress-strain relations are suitably weighted. If m is the proportion of the strain increment required to cause yield in an element during that increment, the weighted stress-strain relation for the transition region becomes

$$\{d\sigma\} = \left([S] - \frac{(1-m)[S]\{\partial\bar{\sigma}/\partial\sigma\}\lfloor\partial\bar{\sigma}/\partial\sigma\rfloor[S]}{H' + \lfloor\partial\bar{\sigma}/\partial\sigma\rfloor[S]\{\partial\bar{\sigma}/\partial\sigma\}}\right)\{de\} \tag{6}$$

We adopt a similar idea in the use of a piecewise linear representation of the work-hardening curve. Here, because the plastic strains during an increment were larger than the strains that the author had previously observed,[9-12] it was found necessary to obtain a mean value of the slope H' at the corners of the piecewise linear curve.

† The matrix $[p^-]$ will be used to refer to this term in subsequent discussion.

Piecewise Linear Generalized Stress-Strain Relations

The linear relation, Eqs. (5) or (6) can now be used to form linear generalized stress-strain relations for a plate or a shell by integrating through the thickness.

The strain increment at a point in a shell is given by the sum of the midwall and bending component

$$\{de\} = \{d\bar{e}\} + z\{dk\} \tag{7}$$

where $\{d\bar{e}\}$ is the midwall component of the strain increment, $\{dk\}$ is the bending component of the strain increment, and z is the distance from the center of the shell wall.

The increment of the direct $\{dN\}$ and bending $\{dM\}$ stress resultants are given by integrating through the thickness

$$\begin{Bmatrix} dN \\ dM \end{Bmatrix} = \int_{-H}^{H} \begin{Bmatrix} d\sigma \\ z\,d\sigma \end{Bmatrix} dz \tag{8}$$

where H is the half-wall thickness. Substituting Eqs. (5) and (7) in Eq. (8), we obtain

$$\begin{Bmatrix} dN \\ dM \end{Bmatrix} = \int_{-H}^{H} \begin{bmatrix} [p^-] & [p^-]z \\ [p^-]z & [p^-]z^2 \end{bmatrix} dz \begin{Bmatrix} d\bar{e} \\ d\bar{k} \end{Bmatrix} = [D] \begin{Bmatrix} d\bar{e} \\ d\bar{k} \end{Bmatrix} \tag{9}$$

where $[D]$ is the generalized strain to generalized stress transformation matrix. The shell wall is divided into a number of stations through the thickness [i.e., Eq. (11)]. The stress history is kept for each of these stations. The matrix $[p^-]$ is evaluated at the start of each increment for each station and the matrix of Eq. (9) is formed by numerical integration through the thickness.

Axisymmetric Shell Theory

An axisymmetric shell element is shown in Fig. 1. The element has local coordinates x and y. The axis is inclined at an angle θ to the axis of symmetry $\bar{x}$. The tangent to a point of the shell is also shown making an angle ϕ with the local x axis. The global coordinate system is formed by coordinate axes $\bar{x}$ and r. The shell is assumed to have a mean radius of curvature R. The distance along the meridian of the shell is given by s as shown in Fig. 1.

The tangential and normal components of displacement in the shell are u_c and w_c; where the subscript c has been introduced to denote that these displacements are measured in curvilinear coordinates. The meridional and circumferential direct and bending strains e_s, e_ψ, k_s, k_ψ, respectively, are given by

$$e_s = (du_c/ds) + (w_c/R) + \tfrac{1}{2}(\chi_c)^2 \tag{10}$$

$$e_\psi = (u_c/r)\sin(\theta + \phi) + (w_c/r)\cos(\theta + \phi) \tag{11}$$

$$\chi_c = dw_c/ds - u_c/R \tag{12}$$

$$k_s = d\chi/ds = d^2w_c/ds^2 - (1/R)du_c/ds - u_c d(1/R)/ds \tag{13}$$

$$k_\psi = (\sin\theta/r)(dw_c/ds) - u_c/R \tag{14}$$

These equations are obtained from the small displacement shell equations by adding to Eq. (10), the most important nonlinear term because of the rotation in the meridional direction. These equations are appropriate for shells with moderate rotation and small strains.[3] The strains defined in Eqs. (10–14) are now expressed in rectilinear displacements u, w along the local coordinate axes x and y. To a first order, the meridional length s is related to the distance x by

$$ds = dx/\cos\phi \tag{15}$$

The distance s is related to the angle ϕ by

$$\phi = \phi_1 - s/R \tag{16}$$

where ϕ_1 is the angle that the tangent to the shell makes with

the axis of symmetry at nodal point 1. The rectilinear displacements u, w are transformed to the curvilinear displacements u_c, w_c by

$$\begin{Bmatrix} u_c \\ w_c \end{Bmatrix} = \begin{bmatrix} \cos\phi & \sin\phi \\ -\sin\phi & \cos\phi \end{bmatrix} \begin{Bmatrix} u \\ w \end{Bmatrix} \tag{17}$$

Equations (15–17) are substituted in Eqs. (10–14) to write the strains in terms of rectilinear displacements u, w.

$$e_s = \cos^2\phi(du/dx) + \sin\phi\cos\phi(dw/dx) + \tfrac{1}{2}\chi^2 \tag{18}$$

$$e_\psi = (u\sin\theta/r) + (w/r)\cos\theta \tag{19}$$

$$\chi = [-\sin\phi\ \cos\phi] \begin{Bmatrix} du/ds \\ dw/dx \end{Bmatrix} \cos\phi \tag{20}$$

$$k_s = \frac{\cos\phi}{R}[\cos\phi\ \sin\phi] \begin{Bmatrix} du/dx \\ dw/dx \end{Bmatrix} + \cos^2\phi[-\sin\phi\ \cos\phi] \begin{Bmatrix} d^2u/dx^2 \\ d^2w/dx^2 \end{Bmatrix} \tag{21}$$

$$[\beta^s] = \begin{bmatrix} 0 & 1 & 0 \\ \dfrac{\sin\theta}{r} & \dfrac{x\sin\theta}{r} & \dfrac{\cos\theta}{r} \\ 0 & \dfrac{1}{R} & 0 \\ 0 & \dfrac{-\phi\sin\theta}{r} & 0 \end{bmatrix}$$

$$k_\psi = \frac{\sin\phi\cos\phi}{r}[-\sin\phi\ \cos\phi] \begin{Bmatrix} du/dx \\ dw/dx \end{Bmatrix} \tag{22}$$

Shell Displacements

The shell displacements are written in local rectilinear coordinates. The shell displacements are represented by three degrees of freedom at a node, two translations and a rotation. The six degrees of freedom connected with the nodes of the element are written as the displacement vector $\{u\}$. Following Khojasteh-Bakht,[14] the shell is assumed to deform according to the displacements

$$u = a_1 + a_2x \tag{23}$$

$$w = a_3 + a_4x + a_5x^2 + a_6x^3 \tag{24}$$

where $a_1, a_2, \ldots, a_6$ are the generalized displacements $\{a\}$. This displacement function allows rigid body motion without inducing strains. The generalized displacements $\{a\}$ are related to the nodal point displacements $\{u\}$ by substituting the coordinates of nodal points 1 and 2 in Eqs. (20, 23, and 24).

$$\begin{Bmatrix} u_1 \\ w_1 \\ \chi_1 \\ u_2 \\ w_2 \\ \chi_2 \end{Bmatrix} = \begin{bmatrix} 1 & & & & & \\ 0 & 0 & 1 & & & \\ 0 & -\sin\phi_1 & 0 & 1 & & \\ 1 & x_2 & & & & \\ 0 & 0 & 1 & x_2 & x_2^2 & x_2^3 \\ 0 & -\sin\phi_2 & 0 & 1 & 2x_2 & 3x_2^2 \end{bmatrix} \{a\} \tag{25}$$

The nodal point displacement to generalized displacement transformation matrix $[\alpha]$ is obtained by inversion of Eq. (25).

$$\{a\} = [\alpha]\{u\} \tag{26}$$

Assuming that changes in $[\alpha]$ may be neglected during an increment of load, we obtain

$$\Delta\{a\} = [\alpha]\Delta\{u\} \tag{27}$$

where the prefix Δ denotes an increment in the quantity concerned. This assumption is equivalent to neglecting the stretching of the element during an increment.

Next obtain the generalized displacement to strain increment transformation matrix $[\beta]$. This is the so-called differential operator of Ref. 21 which now also contains displacement terms due to the use of second-order strain terms. This matrix may be split into two matrices $[\beta^s]$, $[\beta^l]$ containing first-order and second-order displacement terms, respectively,

$$\Delta\{e\} = [\beta]\Delta\{a\} = ([\beta^s] + [\beta^l])\Delta\{a\} \tag{28}$$

We obtain the differential operator $[\beta]$ by substituting Eqs. (23) and (24) in the incremental form of Eqs. (18–22). In the following equations, we have assumed that the angle ϕ is small so that $\sin\phi \simeq \phi$ and $\cos\phi \simeq 1$. With the definition of the strain vector,

$$[e] = [e_s e_\psi k_s k_\psi] \tag{29}$$

we have

$$\begin{bmatrix} \phi & 2\phi x & 3\phi x^2 \\ \dfrac{x\cos\theta}{r} & \dfrac{x^2\cos\theta}{r} & \dfrac{x^3\cos\theta}{r} \\ \dfrac{\phi}{R} & \dfrac{2\phi x}{R} + 2 & \dfrac{3\phi x^2}{R} + 6x \\ \dfrac{\sin\theta}{r} & \dfrac{2x\sin\theta}{r} & \dfrac{3x^2\sin\theta}{r} \end{bmatrix} \tag{30}$$

It is assumed that the only second-order term that contributes significantly to the strain is given by Eq. (18). This results in a nonzero first row of the $[\beta^l]$ matrix

$$[\beta^l] = [0\ -\chi\phi\ 0\ \chi\ 2x\chi\ 3x^2\chi] \tag{31}$$

The subscript 1 is used to denote the first row of the matrix.

The displacements $\{u\}$ are now transformed to the displacements $\{u_g\}$ in the global coordinate system. It is here noted that we shall use the transformation matrix $[T]$ corresponding to the displaced position of the shell element. We also assume that the change in the transformation matrix during an increment of load may be neglected, so that

$$\Delta\{u_g\} = [T]\Delta\{u\} \tag{32}$$

Thus, a stress increment by Eqs. (9, 28, and 32) is given by

$$\Delta\{\sigma\} = [D][\beta][\alpha][T]\Delta\{u_g\} \tag{33}$$

Principle of Virtual Work

The equilibrium equations governing the shell behavior can now be derived. This is achieved in two steps. First, the equivalent nodal forces for an element are defined by the principle of virtual work. The equilibrium equations are then obtained by superposition in the usual manner of the matrix displacement method. This last step is assumed to be well known and is not given here. For brevity, the pressure and body force loads are not included in the following discussion. The pressure and body force loads are assumed to be converted to nodal point loads in a similar consistent manner by the principle of virtual work. The derivation is based on the current *deformed position* of the shell element. Let there be an arbitrary and nonzero virtual displacement $\delta[u]_g$ about the deformed position which results in a virtual strain $\delta[e]$. The δ prefix denotes a virtual change in the quantity concerned.

The equivalent nodal forces $\{P\}$ of the element is then defined by the principle of virtual work,

$$\delta[u_g]\{P\} = \int_A \delta[e]\{\sigma\}dA = \int_A \delta[u_g][T]^T[\alpha]^T[\beta]^T\{\sigma\}dA \tag{34}$$

where A is the surface area of the shell. (The integration of energy through the thickness is already accounted for in the generalized stresses and strains.) Because the virtual displacement $[\delta u_g]$ is arbitrary and nonzero, it may be cancelled from both sides of Eq. (34). This results in a nonlinear matrix equation for the equivalent nodal forces $\{P\}$,

$$\{P\} = \int_A [T]^T[\alpha]^T[\beta]^T\{\sigma\}dA \tag{35}$$

Equation (35) is now linearized by writing it in the form of an implicit differential and making use of Eq. (33),

$$\Delta\{P\} = \int_A \Delta[T]^T[\alpha]^T[\beta]^T\{\sigma\}dA + \int_A [T]^T[\alpha]^T\Delta \times [\beta]^T\{\sigma\}dA + \int_A [T]^T[\alpha]^T[\beta]^T[D][\beta][\alpha][T]\Delta\{u_g\}dA \tag{36}$$

Because of the earlier assumption that the change in the transformation matrix, $\Delta[T]$ may be neglected, the first term on the right-hand side of Eq. (36) may be neglected. The reader should note that the principle of virtual work is based on the current position of the element. If the transformation matrix $[T]$ had been based on the original position instead of the current position, the first term on the right of Eq. (36) cannot be neglected and we would obtain the so-called geometric stiffness of Argyris et al.[22,23] (multiplied by the displacement increment). The second term results in the well-known initial stress matrix[24] whereas the third term accounts for the effect of the increment of strain and may be split into components which account for first-order or second-order displacement terms in the strain displacement relations by the use of Eq. (28).

$$\begin{aligned}\int_A [T]^T[\alpha]^T[\beta]^T[D][\beta][\alpha][T]dA\,\Delta\{u_g\} = {} & \int_A [T]^T[\alpha]^T[\beta^l]^T[D][\beta^s][\alpha][T]dA\,\Delta\{u_g\} + \\ & \int_A [T]^T[\alpha]^T[\beta^s]^T[D][\beta^l][\alpha][T]dA\,\Delta\{u_g\} + \\ & \int_A [T]^T[\alpha]^T[\beta^l]^T[D][\beta^l][\alpha][T]dA\,\Delta\{u_g\} + \\ & \int_A [T]^T[\alpha]^T[\beta^s]^T[D][\beta^s][\alpha][T]dA\,\Delta\{u_g\} = \\ & [k^{(2)}]\Delta\{u_g\} + [k^{(0)}]\Delta\{u_g\}\end{aligned} \tag{37}$$

The first three terms have been collected together in $[k^{(2)}]$ and will be called the initial displacement matrix.[16] If the current stress-strain relation is of the same order as its original elastic value, the initial displacement matrix will be of the same order as the initial stress matrix. In this connection, it is relevant to note that the values of the incremental elastic-plastic stress-strain relations were found to be of the same order as the original elastic values.[25] It is therefore thought that the initial displacement analysis will play as significant a role in large displacement analysis as the initial stress matrix. Reference[16] already gives some examples illustrating the importance of the initial displacement matrix in truss and beam element analysis. Further examples are being collected for other elements and this will form the subject of a later note. For the present, it is sufficient to note that the initial displacement matrix should be included in any large displacement analysis since it is called for in Eq. (37). In addition it should be noted that this term exists regardless of whether a fixed or a moving coordinate system is used.

In general, the stiffness matrices $[k^{(0)}]$ and $[k^{(2)}]$ are not separated. However, in cases where eigenvalue solutions are required for geometry sensitive shells, these terms are separated to give the eigenvalue problem,

$$[k^{(0)}]\Delta\{u_g\} + \lambda([k^{(1)}] + [k^{(2)}])\Delta\{u_g\} = 0 \tag{38}$$

The element stiffness matrices described here are formed by numerical integration. A general outline of the computer program used will be given in a later section.

Initial Stress Matrix

In this section, we outline a method for conveniently assembling the initial stress matrix. Alternative methods exist and have been described by other authors.[22,24,26] The method presented here is one which the author has found very general and straightforward. It is easily implemented in a computer program of the type used here.

The initial stress term can be broken down into a summation of the m stress components.

$$\int_A [T]^T[\alpha]^T\Delta[\beta]^T\{\sigma\}dA = \sum_{i=1}^{m} \int_A \sigma_i [T]^T[\alpha]^T\Delta\{\beta_i{}^T\}dA \tag{39}$$

where i is the index of the stress components and $\{\beta_i{}^T\}$ is the transpose of the corresponding ith row of the matrix $[\beta]$.

The increment $\Delta\{\beta_i{}^T\}$ is now written as a partial differential of the large displacement quantities p_j in the incremental strain displacement relations in the $[\beta]$ matrix

$$\Delta\{\beta_i{}^T\} = \{\partial\beta_i{}^T/\partial p_j\}\,[\partial p_j/\partial[a]]\Delta\{a\} \tag{40}$$

where $j = 1$ to number of large displacement quantities. In the shell problem, the rotation χ is the only large displacement quantity appearing in the $[\beta]$ matrix. In addition, this term only appears in the first row of the $[\beta]$ matrix [Eq. (31)]. Because of the partial differentiation, we note that only the large displacement component of the matrix $[\beta^l]$ is concerned in Eq. (40). Hence with $p_1 = \chi$ and $m = 1$, and using Eq. (31) in Eq. (40), we obtain

$$\Delta\{\beta_1{}^T\} = \Delta\{\beta_1{}^{lT}\} = \Delta\left\{\frac{\partial\beta_1{}^{lT}}{\partial\chi}\right\}\left[\frac{\partial\chi}{\partial[a]}\right]\Delta\{a\} = \begin{Bmatrix}0\\-\phi\\0\\1\\2x\\3x^2\end{Bmatrix}[0\ -\phi\ 0\ 1\ 2x\ 3x^2]\Delta\{a\} \tag{41}$$

Computer Program

The aforementioned theory was implemented in a finite element computer program. A previously developed general purpose program which formed the element stiffness by integration was used as a starting point.

The advantage of using a numerical integration to form the stiffness matrices was very clear. Subroutines had only to be written to form the $[\alpha]$ $[\beta^s][\beta^l]$ and $[T]$ matrices. The integration and assembly of the master stiffness matrices were then carried out automatically by the computer. The program in its original form solved the matrix equations by an iterative over-relaxation process. Convergence in the shell examples was found to be extremely slow. It was decided to use a direct solution instead of an iterative one. A direct solution using a submatrix form of the Crout-Banachiewicz reduction procedure was developed. This follows the usual elimination procedure with the difference that the operations are now made on small submatrices of the order of the number of degrees of freedom per nodal point. Thus, the subroutine which effects the direct solution only stores nonzero elements and the submatrix form of the solution reduced the total indexing and search of the nonzero elements. A direct Cholesky solution which only stores nonzero elements has been described by Melosh et al.[27] It was there noted that calculations restricted to nonzero elements resulted in a significant saving of computing time.

The midway point of the shell element was used as its representative point for evaluating stresses. This and the use of a constant shell element radius R required smaller elements to be used in regions of large bending. The stresses were evaluated at 11 points through the thickness. Figure 2 gives a schematic of the flow of the general purpose program.

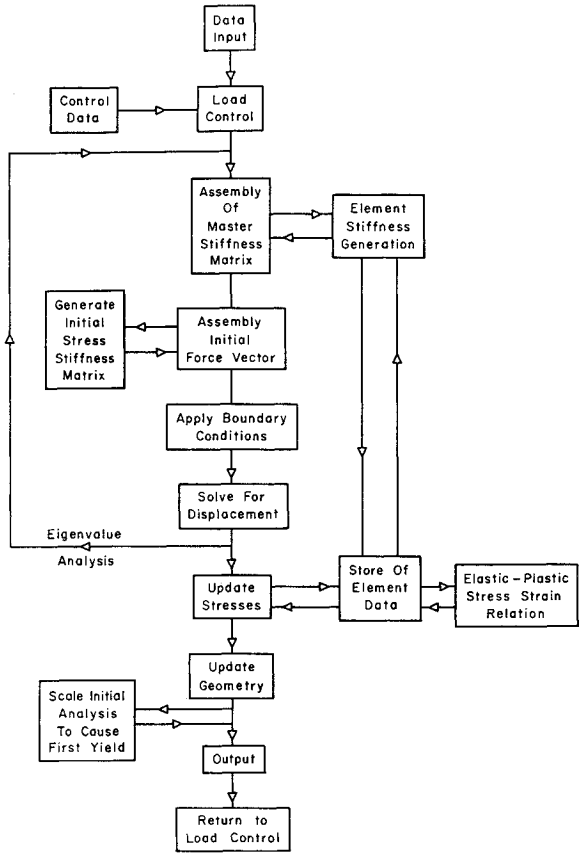

Fig. 2 Flow chart for computer program.

Results

In order to check the theory, calculations were carried out for a toroidal pressure vessel under internal pressure, centrally loaded spherical shells and oblate spheres under external pressure.

The torispherical head (Fig. 3) was tested by Stoddart and Owen.[28] The vessel was made of a mild steel with a yield stress of 40,197 lb/in.^{2}. A Young's Modulus of 30.354×10^6 lb/in.^{2}, and a Poisson's ratio of 0.31 were reported by Stoddart and Owen.

The spherical vessels (Fig. 4) tested by Leckie and Penny[29] were made of Duralumin. The vessels were machined with a central boss attached to the spherical shell. The nominal radius and thickness were 3 and 0.05 in., respectively. A yield stress of 41,000 lb/in.^{2} was used with a piecewise linear work hardening curve which consisted of slopes $2.5\frac{5}{4} \times 10^5$, 0.0 lb/in.^{2} at break-points of equivalent plastic strain of 0.0 and 2.0%, respectively. Young's Modulus was estimated to be 10×10^6 lb/in.^{2} from the stress-strain curve in Ref. 29.

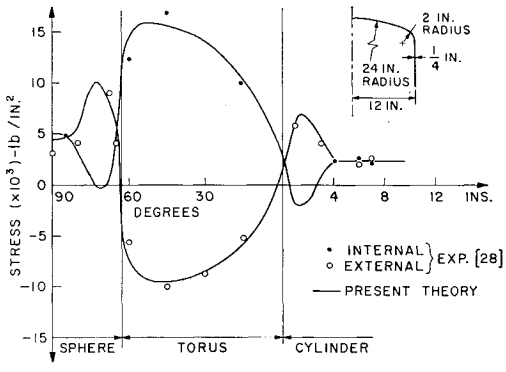

Fig. 3 Stress distribution for torispherical vessel.

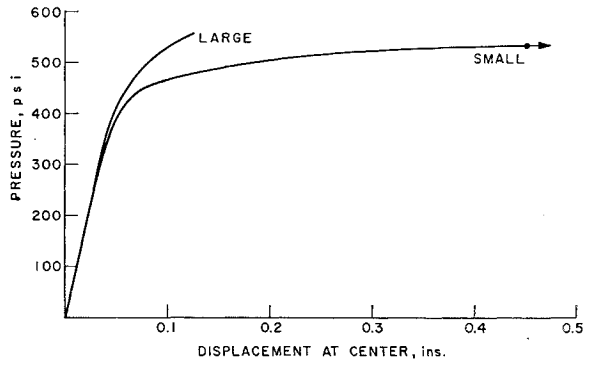

Fig. 4 Pressure-displacement at center.

The oblate spherical shell analyzed with elastic theory by Bushnell[2] is shown in Fig. 5. A dimensionless yield stress of $0.00666E$ was used, together with a linear work-hardening curve with a slope of $0.05E$. This corresponds roughly to the stress-strain curve of an aluminum alloy.

Case Studies

1. Torispherical Pressure Vessel under Internal Pressure

As a first test case, numerical results were obtained for comparison with the experimental results for a torispherical pressure vessel under internal pressure tested by Stoddart and Owen.[28] Two separate analyses were performed for the torisphere. The program was first run without the large displacement terms. The second analysis included the large displacement terms. These results are labelled small and large, respectively. Figure 3 gives the elastic stress distribution in the meridional direction for a pressure of 100 psi. There is reasonable agreement with experiment. Figure 6 gives a plot of the pressure-maximum strain (at station 45° in the torisphere). The experimental results of Stoddart and Owen[28] and the numerical results of Marcal and Pilgrim[10] are shown also. Good agreement is found between the results. The present small displacement results agree well with the results of Ref. 10. The results for the large displacement solutions are in good agreement with the experimental results. Figure 5 shows the pressure-central displacement plot for the small and large displacement analyses.

It is noted that, in the case of the small displacement analysis and that of Ref. 10 an upper limit load was reached. In the present large displacement analysis, this upper limit was not reached. It appeared that further load could be applied to the vessel, albeit at the penalty of large strains at the knuckle and large over-all deflections. This behavior is consistent with the picture of a mild steel vessel being able to

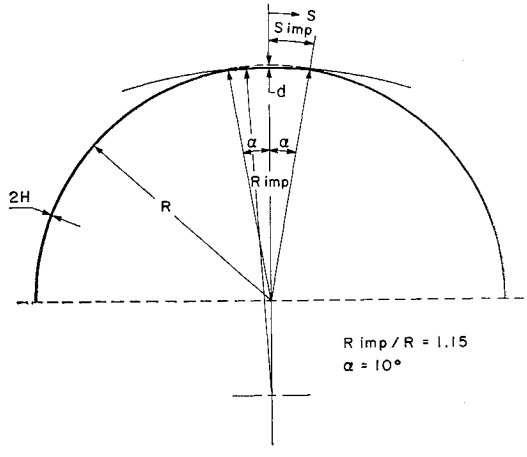

Fig. 5 Externally pressurized imperfect hemisphere.

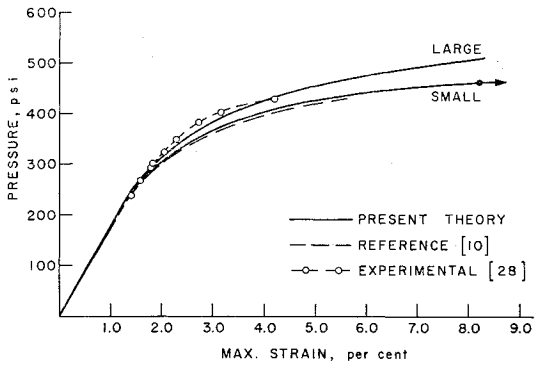

Fig. 6 Pressure-maximum strain in torisphere.

withstand pressures considerably above its first yield. This is due to work-hardening as well as geometry changes. In the present analysis, since an elastic-perfectly plastic material was assumed, the ability of the vessel to withstand pressures above the theoretical small displacement limit load is confirmation of the strengthening due to a change of geometry.

2. Spherical Shells with a Central Load

Figure 7 shows the spherical vessels treated by Leckie and Penny.[29] A central load was applied at the apex of the shell via a boss which was integrally machined with the shell. Figure 8 gives the load-relative displacement of the boss for four shells with a constant radius and four different boss sizes. The experimental buckling loads obtained in Ref. 29 are shown also. There is fair agreement between the present results and the experiment. It is thought that the comparison is prejudiced by the assumption of a built-in shell at the shell-boss junction. The stresses at the junction are thought to be less severe. It is noted that excellent agreement was obtained for the case where the boss radius was very small. In this case, the boundary condition at the shell-boss junction most closely resembles that of a built-in shell.

3. Spherical Shells with Imperfections under External Pressure

Bushnell[2] analyzed oblate spheres under external pressure. In Ref. 2, it was noted that the stresses at collapse were too high to remain elastic. It was therefore thought useful to study the effect of plastic yielding on the behavior of the shells. Figure 5 shows the oblate spherical shell with thickness $2H$ and the axisymmetric imperfection over the angle α.

Figure 9 gives a comparison between the buckling pressure of the elastic shell of[2] and the present elastic-plastic results. The results are plotted in terms of the parameters used in Ref. 2. The classical buckling load p_c is defined by

$$p_c = 1.21(2H/R)^2E \qquad (42)$$

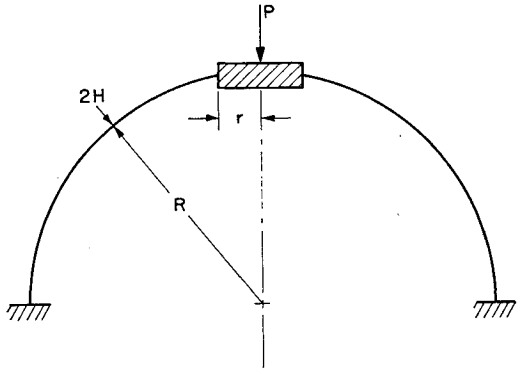

Fig. 7 Shell geometry.

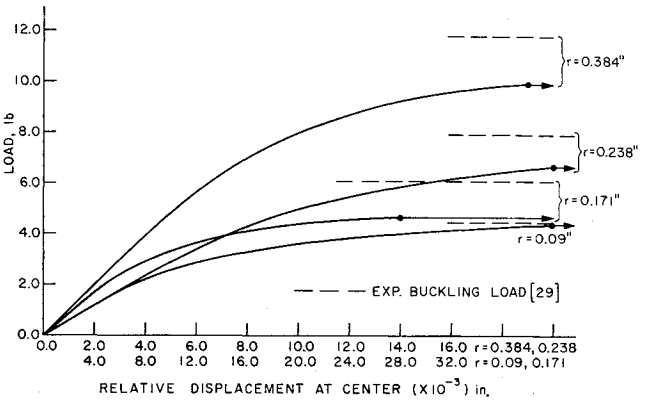

Fig. 8 Load-relative displacement at center.

where E is the Young's modulus, R is the radius of the sphere. The geometric parameter λ is defined by

$$\lambda = [12(1 - \nu^2)]^{1/4}(R/2H)^{1/2}(R/R_{\text{imp}})\alpha \qquad (43)$$

where R_{imp} = mean radius of the flattened portion of the sphere.

Plastic yielding has a considerable effect on the behavior of the oblate shells under external pressure. This effect increases with the thickness to radius ratio. It is noted that the failures at the higher thickness to radius ratios ($\lambda \simeq 1.5$) are due to membrane yield.

Discussion

The present analysis has been applied to a sufficiently wide sample of shell types to enable some opinion to be offered on its accuracy. It is seen from the case study of the torisphere

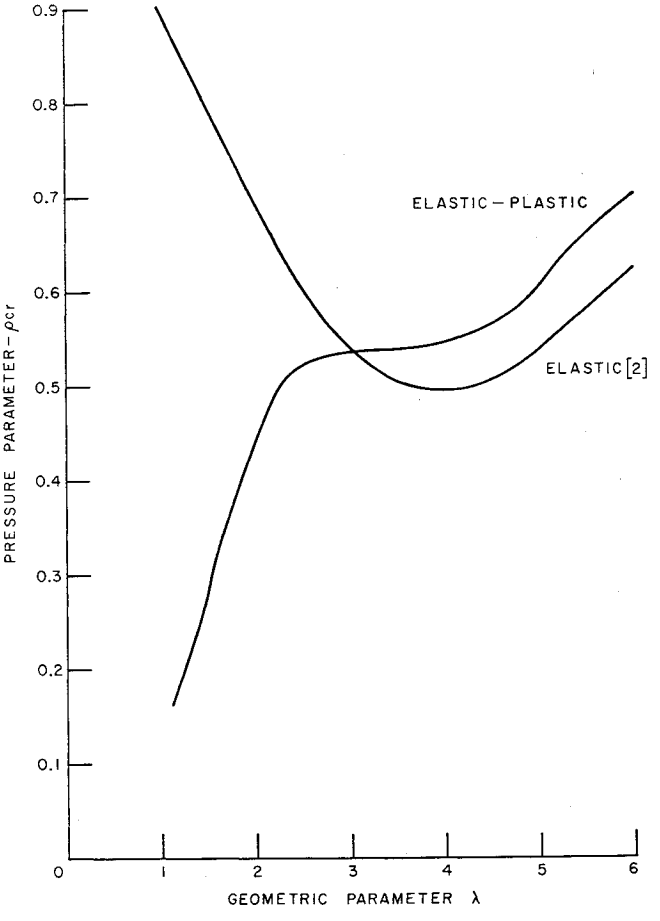

Fig. 9 Buckling pressure for oblate shells, $R_{\text{imp}}/R = 1.15$.

that the analysis for the large displacement elastic-plastic shell results in an overestimate of the load to cause large strains by about 5–10%. It is thought that this may be caused by the assumption that at any position through the shell thickness the stress state in the element may be represented by its centroidal value. Although this may adequately define a stress level, it is thought that it may also imply a certain restriction on the straining of the shell due to the normal plastic flow rule. Fortunately, the nonlinear geometric and material behavior interact so strongly that 8% may be thought of as a reasonable estimate of the error on the buckling load.

The case studies of the centrally loaded sphere bring out the importance of the correct boundary conditions. A better analysis of the shells with larger boss radius will depend on the development of an analysis with combined axisymmetric solid body and shell elements.[30]

It is generally difficult to detail the actual steps taken to implement a theory in terms of a computer program. For this reason, it is important to note that in the present case it was found that the inclusion of the large displacement theory could be made modular, after which the combination with the other modular aspects of the finite element analysis was accomplished with ease. Now that the program module for large displacement analysis exists, it is thought that the current analysis may be extended to other plate and shell elements.

Conclusions

A large displacement, elastic-plastic finite element analysis has been developed for the general axisymmetric shell of revolution. Results were obtained for various shells and comparisons were made with theory and experiment. Reasonable agreement was found.

A study was then made of the effect of plastic yielding on oblate spherical shells under external pressure. Comparisons were made with the elastic buckling loads obtained by Bushnell.[2] It was found that plastic yielding had a considerable effect on the buckling load of these shells and that this effect was more marked in the thicker shells.

References

[1] Thurston, G. A. and Penning, F. A., "Effect of Axisymmetric Imperfections on the Buckling of Spherical Caps under Uniform Pressure," *AIAA Journal*, Vol. 4, No. 2, Feb. 1966, pp. 319–327.

[2] Bushnell, D., "Nonlinear Axisymmetric Behavior of Shells of Revolution," *AIAA Journal*, Vol. 5, No. 3, March 1967, pp. 432–439.

[3] Navaratna, D. R., Pian, T. H. H., and Witmer, E. A., "Analysis of Elastic Stability of Shells of Revolution by the Finite Element Method," *Proceedings of the ASME*, March 1967, pp. 175–186.

[4] Cohen, G. A., "Computer Analysis of Asymmetric Buckling of Ring-Stiffened Orthotropic Shells of Revolution," *AIAA Journal*, Vol. 6, No. 1, Jan. 1968, pp. 141–149.

[5] Krenzke, M. A. and Kiernan, T. J., "The Effect of Initial Imperfections on the Collapse Strength of Deep Spherical Shells," DTMB 1757, Feb. 1965, David Taylor Model Basin.

[6] Bijlaard, P. P., "Theory and Tests on the Plastic Stability of Plates and Shells," *Journal of the Aerospace Sciences*, Vol. 16, No. 9, 1949.

[7] Lee, L. H. N., "Inelastic Buckling of Initially Imperfect Cylindrical Shells Subject to Axial Compression," *Journal of the Aerospace Sciences*, Vol. 29, 1962, pp. 87–95.

[8] Batterman, S. C., "Plastic Buckling of Axially Compressed Cylindrical Shells," *AIAA Journal*, Vol. 3, No. 3, March 1965, pp. 316–325.

[9] Marcal, P. V. and Turner, C. E., "Elastic-Plastic Behavior of Axisymmetrically Loaded Shells of Revolution," *Journal of Mechanical Engineering Science*, Vol. 5, No. 3, 1963, p. 232.

[10] Marcal, P. V. and Pilgrim, W. R., "Stiffness Method for Elastic-Plastic Shells of Revolution," *Journal of Strain Analysis*, Vol. 1, 1966, p. 339.

[11] Marcal, P. V., "Elastic-Plastic Behavior of Pipe-Bends with In-Plane Bending," *Journal of Strain Analysis*, Vol. 2, No. 1, 1967, pp. 84–90.

[12] Marcal, P. V. and Turner, C. E., "Elastic-Plastic Behavior of Flush Nozzles in Spherical Pressure Vessels," *Journal of Mechanical Engineering Science*, Vol. 9, No. 3, 1967, pp. 162–189.

[13] Marcal, P. V. and Turner, C. E., "Limited Life of Shells of Revolution Subjected to Severe Local Bending," *Journal of Mechanical Engineering Science*, Vol. 7, No. 4, 1965, pp. 408–423.

[14] Khojasteh-Bakht, M., "Analysis of Elastic-Plastic Shells of Revolution Under Axisymmetric Loading by the Finite Element Method," Ph.D. dissertation, SESM 67-8, April 1967, Univ. of California at Berkeley.

[15] Kalnins, A., "Analysis of Shells of Revolution Subjected to Symmetrical and Non-Symmetrical Loads," *Journal of Applied Mechanics*, Vol. 31, 1964, pp. 467–476.

[16] Marcal, P. V., "The Effect of Initial Displacements on Problems of Large Deflection and Stability," Engineering Report ARPA E54, Nov. 1967, Brown Univ.

[17] Yamada, Y., Yoshimura, N., and Sakurai, T., "Plastic Stress-Strain Matrix and its Application for the Solution of Elastic-Plastic Problems by the Finite Element Method," Report of the Institute of Industrial Science, Aug. 1967, Univ. of Tokyo.

[18] Rice, J. R., private communication, Brown University, March 1968.

[19] Pope, G., "A Discrete Element Method for Analysis of Plane Elastic-Plastic Stress Problems," TR 65028, 1965, Royal Aeronautical Establishment.

[20] Swedlow, J. L. and Yang, W. H., "Stiffness Analysis of Elastic-Plastic Plates," SM 65-10, 1965, Graduate Aeronautical Lab., California Institute of Technology.

[21] Clough, R. W., "The Finite Element Method in Structural Mechanics," *Stress Analysis*, edited by O. C. Zienkiewicz and G. S. Holister, Wiley, New York, 1965, Chap. 7.

[22] Argyris, J. H., Kelsey, S., and Kamel, H., *Matrix Methods of Structural Analysis*, AGARDograph No. 72, Pergamon Press, New York, 1964, pp. 105–120.

[23] Zienkiewicz, O. C., "Non-Linear Problems," *The Finite Element Method in Structural Mechanics*, 1967, Chap. 10.

[24] Martin, H. C., "On the Derivation of Stiffness Matrices for the Analysis of Large Deflection and Stability Problems," *Proceedings 1st Conference on Matrix Methods in Structural Mechanics*, AFFDL-TR-66-80, 1966, pp. 697–715.

[25] Marcal, P. V., "A Stiffness Method for Elastic-Plastic Problems," *International Journal of Mechanical Sciences*, Vol. 7, 1965, pp. 229–238.

[26] Kapur, K. K. and Hartz, B. J., "Stability of Plates Using the Finite Element Method," *Proceedings of American Society of Civil Engineers*, Vol. 92, No. EM2, 1966, pp. 177–195.

[27] Melosh, R. et al., "Computer Analysis of Large Structural Systems," AIAA Paper 67-955, Anaheim, Calif., 1967.

[28] Stoddart, J. S. and Owen, B. S., "Stresses in a Torispherical Pressure Vessel Head," Meeting on Stress Analysis Today, 1965, Stress Analysis Group, Institute of Physics.

[29] Leckie, F. A. and Penny, R. K., "Plastic Instability of a Spherical Shell," *Engineering Plasticity*, edited by J. Heyman and F. A. Leckie, Cambridge University Press, 1968, pp. 401–411.

[30] Jones, R. E. and Strome, D. R., "A Survey of Analysis of Shells by the Displacement Method," *Proceedings 1st Conference Matrix Methods in Structural Mechanics*, AFFDL-TR-66-80, 1966, pp. 205–229.